WWW.IJRPR.COM

**International Journal of Research Publication and Reviews**

Journal homepage: www.ijrpr.com ISSN 2582-7421

# Formulation and evaluation of liposomes for antiacne activity of Resveratrol

***Harsimran Singh[1], Monika Bansal[2], Jasleen Kaur[3]***

Akal College of Pharmacy & Technical Education, Mastuana Sahib, Sangrur, India – 148 001
Corresponding author:
Mrs. Monika Bansal; Associate Professor
E mail: monikabansal8@gmail.com

**ABSTRACT :**

The development and characterization of liposomal resveratrol represent a significant advancement in overcoming the pharmacological limitations of resveratrol, a naturally occurring polyphenol various medicinal properties. Despite its therapeutic potential, resveratrol's clinical utility is hindered by poor aqueous solubility, rapid metabolism, low oral bioavailability, and susceptibility to degradation. Liposomal encapsulation has emerged as a promising strategy to enhance resveratrol's stability, solubility, and targeted delivery, thereby improving its therapeutic efficacy. This comprehensive approach involved the formulation, optimization, and detailed characterization of resveratrol-loaded liposomes to ensure their suitability for biomedical applications. In conclusion, the development and characterization of liposomal resveratrol have successfully addressed the major challenges associated with resveratrol's delivery and therapeutic application. By encapsulating resveratrol within liposomes, its solubility, stability, and bioavailability were significantly improved, while the sustained and targeted release profiles enhanced its pharmacological efficacy. The rigorous characterization of particle size, zeta potential, encapsulation efficiency, and in vitro release provided a solid foundation for the formulation's optimization and scalability. These advancements position liposomal resveratrol as a promising candidate for clinical translation, offering potential benefits in treating conditions such as cancer, cardiovascular diseases, and neurodegenerative disorders. Future research should focus on scaling up production, conducting long-term toxicity studies, and exploring clinical trials to validate the safety and efficacy of liposomal resveratrol in humans. Overall, this work exemplifies the potential of nanotechnology to revolutionize the delivery of poorly soluble phytochemicals, paving the way for their broader clinical application.

## Introduction

### *Liposomes:*

Liposomes are spherical particles with one or more bilayer membranes composed of phospholipids. These bilayers encapsulate an aqueous core, and the medium inside and outside the liposome can differ and be altered (e.g., via microinjection or dialysis). Lipid molecules, consisting of hydrophilic headgroups and hydrophobic tails, self-assemble into bilayers when their solubility in water decreases. Unlike ordinary amphiphiles with higher critical micelle concentrations (CMCs), bilayer-forming lipids have extremely low CMCs, indicating very low water solubility (Chatterjee at al., 2002). In this process, hydrophilic headgroups face outward to the aqueous phase, while hydrophobic tails interact within the bilayer, minimizing free energy. Liposomes are analogs of natural membranes and are typically formed via the spontaneous self-organization of pure lipids or lipid mixtures. This characteristic makes them valuable in bottom-up engineering approaches (Shimomura et al., 2001).

***Types of Liposomes:***

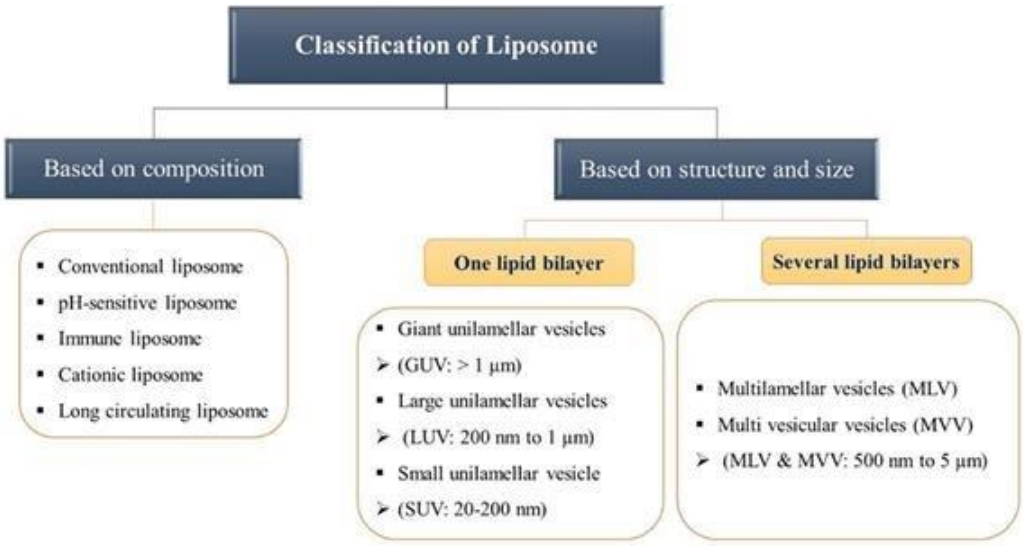


**Figure: General classification of liposomes**

**1. *Conventional Liposomes***

Conventional liposomes are synthesized using natural or synthetic phospholipids, with or without cholesterol, representing the first generation of liposomal formulations (Bangham, 1961). Cholesterol is often added to enhance liposome stability by improving membrane fluidity and modifying bilayer rigidity. Wu et al. reported that incorporating cholesterol into liposomes composed of hydrogenated soybean phospholipids (HSPC) and DSPE-PEG2000 reduced membrane rigidity. Notably, liposomes with moderate rigidity demonstrated superior tumor penetration and enhanced anti-tumor efficacy (Wu et al., 2019). Similarly, Kaddah et al. studied the effect of cholesterol content on the permeability and fluidity of DPPC liposome membranes. They found that higher cholesterol concentrations increased the average size of liposomes, causing a shape transition from irregular to nanosized, uniform, and spherical vesicles. Additionally, cholesterol reduced bilayer fluidity and influenced the release of hydrophilic molecules from lipid vesicles (Kaddah et al., 2018).

**2. *Charged Liposomes:***

Oleic acid and N-[1(2,3-dioleoyloxy)propyl]-N,N,N-trimethylammonium chloride (DOTAP) are commonly used to produce anionic and cationic liposomes, respectively. Charged liposomes exhibit greater stability during storage, as the electrostatic repulsion between charged particles minimizes aggregation. Cationic liposomes are widely employed in gene therapy due to their ability to effectively encapsulate nucleic acids through electrostatic interactions (Jovanović et al., 2017). These liposomes are particularly well-suited for delivering negatively charged macromolecules such as DNA, RNA, and oligonucleotides, as their negative charge and large size typically prevent passive diffusion into cells. Additionally, cationic liposomes demonstrate selective targeting of angiogenic endothelial cells in tumors and are considered promising for delivering therapeutics to the brain (Majzoub et al., 2016; Dass et al., 2003). They can cross the blood-brain barrier (BBB) via receptor-mediated or absorptive-mediated transcytosis. In contrast, anionic liposomes are less stable in the bloodstream compared to their neutral and cationic counterparts, exhibiting higher clearance rates. However, they are commonly utilized in transdermal drug delivery systems due to their ability to enhance penetration through the stratum corneum of the skin (Lai et al., 2021).

**3. *Stealth-Stabilized Liposomes***

Second-generation liposomes, known as stealth liposomes, are modified with surface decorations such as synthetic polymers, glycoproteins, polysaccharides, or receptor-specific ligands to improve distribution and promote accumulation at target sites (Hervé et al., 2008; Youn et al., 2014). Hyaluronic acid, polyvinyl alcohol (PVA), and polyethylene glycol (PEG) are commonly used for steric stabilization, with PEGylation being the most widely adopted approach. PEGylated liposomes, often referred to as stealth liposomes, are designed to evade immune detection. The first successful PEGylated liposome-based product, Doxil®, demonstrated the advantages of this approach. Stealth-stabilized liposomes exhibit prolonged circulation times, enabling better accumulation at targeted sites compared to conventional liposomal drugs (Carthy et al., 2015; Knudsen et al., 2015).

**4. *Actively-Targeted Liposomes***

Actively-targeted liposomes, categorized as third-generation liposomes, are designed to enhance the selective interaction of liposomes with diseased cells. This approach facilitates receptor-mediated endocytosis, enabling the delivery of the liposome and its payload directly into the target cells (Semple et al., 1998; Suk., et al., 2016).

While many liposomal nanocarriers for anti-tumor drug delivery rely on passive targeting through the enhanced permeability and retention (EPR) effect of cancerous cells, this method does not distinguish between healthy and diseased cells. To address this limitation, cell-specific targeting liposomes

have been developed to improve the accumulation and localization of therapeutic agents in diseased tissues (Gregoriadis et al., 1974; Gonzalez-Rodriguez et al., 2011).

Targeting can be further enhanced by incorporating molecular recognition moieties, allowing for more efficient drug delivery with reduced side effects. Examples of these targeting strategies include the use of simple peptides, proteins (such as antibodies) or their fragments carbohydrates, nucleic acids, or vitamins (Allen., et al., 2013; He et al., 2018; Vaage et al., 1993).

### 5. *Stimuli-Responsive Liposomes*

Stimuli-responsive liposomes are advanced, "smart" liposomal systems designed to release their drug payload rapidly in response to specific physicochemical or biochemical triggers, such as changes in pH, temperature, redox potential, enzyme concentration, or exposure to ultrasound, electric, or magnetic fields.

These liposomes are engineered with specific components that regulate the stability and permeability of the lipid bilayer. Stimuli can be categorized into two types: remote and local. Remote stimuli include external factors such as heat, magnetic fields, light, electric fields, and ultrasound. In contrast, local triggers originate within target tissues, such as changes in pH, redox potential or the presence of enzymes.

### 6. *Bubble Liposomes*

Bubble liposomes, also known as gas-encapsulated liposomes, hold significant promise for novel applications in gene and drug delivery systems [145]. Recently, these liposomes have been utilized to encapsulate bioactive gases and/or drugs, enabling ultrasound-controlled drug release and enhanced delivery efficiency [146]. Nitric oxide (NO) bubble liposomes provide a unique approach to intravenous NO therapy, offering advantages over traditional microbubbles. These liposomes shield NO from scavenging by hemoglobin, a challenge commonly faced by free NO in vitro. Similarly, oxygen bubble liposomes (OBLs) facilitate high oxygen concentrations and elevated partial oxygen pressure (pO2) in the lungs. This distinguishes OBLs from conventional fluorocarbon- and hemoglobin-based oxygen transporters, positioning them as effective platforms for sustained oxygen delivery.

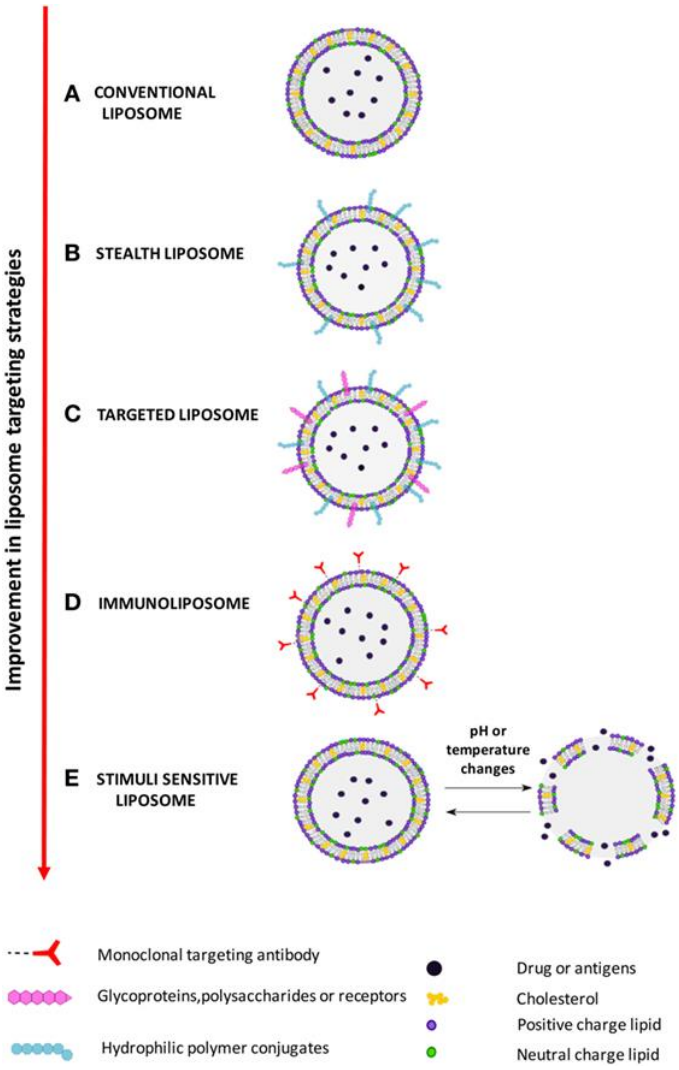


**Figure: Different types of liposomes**

### *1.2. Structural Components of Liposomes*

Liposome vesicles primarily consist of phospholipids, which form the bilayered membrane, and cholesterol, which plays a key role in stabilizing the membrane. The characteristics of liposomes are largely influenced by the type of phospholipids used in their composition.

**1.2.1. Phospholipids**

Phospholipids are amphipathic molecules, meaning they possess both hydrophilic and hydrophobic regions (Federico & Vladimir, 2013; Fahr et al., 2005). Their structure includes a hydrophilic head containing a phosphorus molecule within a phosphoric acid group and two hydrophobic tails consisting of long hydrocarbon chains. Phospholipids are categorized into three main classes: phosphoglycerides, phosphoinositides, and phosphosphingosides.

***A. Phosphoglycerides***

Phosphoglycerides are the most commonly used phospholipids, characterized by a glycerol backbone containing three hydroxyl (OH) groups. Two of these OH groups are linked to fatty acids, while the third is bonded to a phosphoric acid group. The variation in phosphoglycerides arises from the specific polar head alcohol group esterified with phosphoric acid.

All phosphoglycerides possess two nonpolar fatty acid "tails," typically consisting of C16 or C18 carbon chains. One of these fatty acids is saturated, while the other is unsaturated, and the unsaturated fatty acid is always attached to the middle or β-hydroxyl group of glycerol.

A. **Lecithins (Phosphatidylcholines)**

Lecithin, also known as phosphatidylcholine, is a type of phospholipid containing a phosphate group. It is commonly derived from egg yolk or soybean sources. Lecithin is composed of unsaturated nonpolar fatty acids, glycerol, phosphoric acid, and a nitrogenous base, choline.

**B.** ***Cephalins***

Cephalins share a similar fundamental structure with lecithins, except that the choline in lecithins is replaced by either ethanolamine or serine. Examples of cephalins include phosphatidylethanolamine and phosphatidylserine.

Cephalins exist in two forms, α and β, depending on the position of the two attached fatty acids. The primary amino group in ethanolamine is a weaker base compared to the quaternary ammonium group in choline. As a result, cephalins are more acidic and exhibit lower solubility in alcohol compared to lecithins.

**C.** ***Plasmalogens (Phosphoglyceracetals)***

Plasmalogens make up approximately 10% of phospholipids and share a structural similarity with other phosphoglycerides, except that one of the fatty acids is replaced by an unsaturated ether. The nitrogenous base attached to the phosphoric acid in plasmalogens can be choline, ethanolamine, or serine, resulting in different types such as phosphatidal choline, phosphatidal ethanolamine, and phosphatidal serine.

***B. Phosphoinositides (Phosphatidylinositols)***

Phosphoinositides are a class of phospholipids that contain inositol, a cyclic hexahydroxy alcohol, attached to phosphoric acid. Upon hydrolysis, phosphoinositides yield glycerol, fatty acids, inositol, and phosphoric acid in varying amounts (one, two, or three moles). Based on this, they are classified as monophosphoinositide, diphosphoinositide, and triphosphoinositide. Phosphoinositides are also categorized as glycolipids due to the presence of a carbohydrate residue.

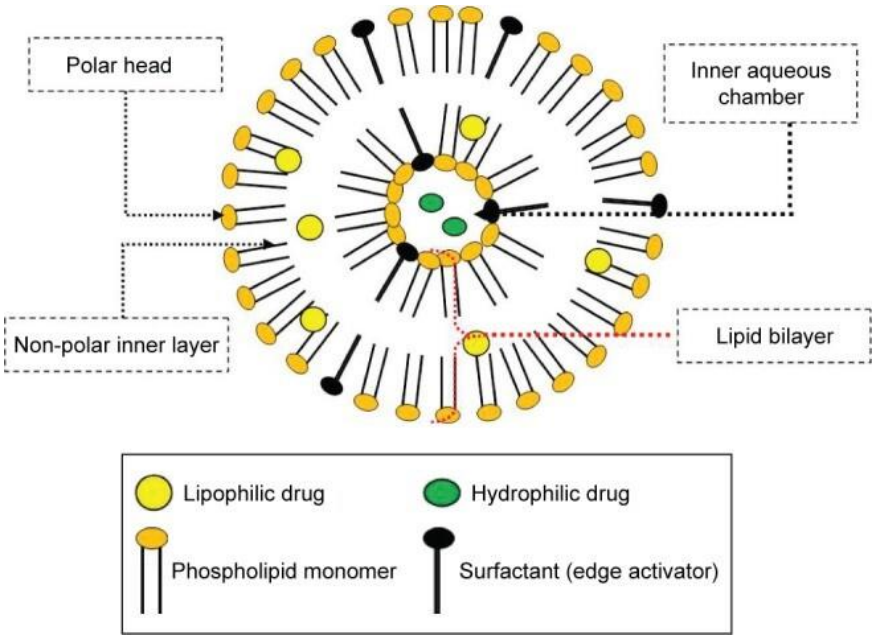

### *1.2 Characterization of the drug*

For the current study, resveratrol was acquired from Yucca Enterprises in Mumbai, India. The drug's specific characteristics were then noted, and the outcomes were then contrasted with established benchmarks found in the literature. The following formulation studies were carried out.

a**) Organoleptic properties**: The drug powder was physically examined to determine its colour, state, and other physical characteristics.

b) **Solubility studies in solvents and excipients**: In 1 millilitre of solvent (methanol, ethanol, Dimethyl sulfoxide (DMSO)) and excipients (phosphatidylcholine, cholesterol and tween 80), 10 milligrams of excess resveratrol was added. At room temperature, all of the samples were shaken for 24 hours. Subsequently, the samples underwent a 10-minute centrifugation at 10,000 rpm, and the supernatant was taken out and filtered using a 0.45-micron filter. At 304 nm, samples were examined using UV spectroscopy after appropriate dilutions were made using appropriate solvents. Solubility was computed using the noted absorbance (Herneisey M et al., 2016; Balata GF et al., 2016).

c) **Identification of drug and analytical methodology:** UV spectrophotometry was used as an analytical method of Resveratrol for identification and to quantify resveratrol for different studies including solubility studies, partition coefficient, in vitro drug release and ex vivo skin permeability studies. Methanol and PBS (pH 5.5) were used.

**1.2) Determination of absorption maxima (λmax) and Calibration curve construction**

- Using a UV spectrophotometer, the produced solution was scanned between 200 and 400 nm to determine the absorption maxima (λmax) of resveratrol, which was then compared with published data.
- The produced dilutions were then scanned using a UV spectrophotometer at the determined absorption maxima (λmax), which is 304 nm, to determine the absorbance. The absorbance and concentration of resveratrol were correlated to create a calibration curve, and linear regression analysis was used to determine the best-fit line.

**2) Construction of calibration curve using Phosphate Buffer Solution(PBS) (pH 5.5)**

**2.1) Preparation of PBS (pH 5.5)**: Using Sorenson's phosphate buffer technique, a PBS solution with a pH of 5.5 was created. To make a 0.2 M solution of disodium hydrogen phosphate, 3.56 g of the substance was first dissolved in 100 ml of distilled water. Likewise, a 0.2 M solution of sodium dihydrogen phosphate was created by dissolving 2.76 g of the compound in 100 ml of distilled water. 4 ml of the 0.2 M disodium hydrogen phosphate solution was added to a beaker and 46 ml of 0.2 M sodium dihydrogen phosphate solution was then added to it. Next, using distilled water, the mixture was diluted to a final volume of 100 ml. A very small amount of sodium dihydrogen phosphate solution was added to fine tune the pH to a desired level.

**2.2) Preparation of stock solution and dilutions:** 10 mg of resveratrol were dissolved in 10 ml of prepared PBS of pH 5.5 to create a stock solution containing one milligram of resveratrol per millilitre that is 1000 mcg/ml. The stock solution was then diluted ten times to create a working standard of 100 mcg/ml.

It was then diluted once more to create a solution with a concentration of 10 mcg/ml. Using this method, further dilutions were made by taking suitable quantities so as to achieve the resultant dilutions of 2, 4, 6, 8 and 10 mcg/ml, respectively.

**2.3) Construction of calibration curve with PBS pH 5.5:** The produced dilutions were then scanned using a UV spectrophotometer at 304 nm, to determine the absorbance. The absorbance and concentration of resveratrol were correlated to create a calibration curve, and linear regression analysis was used to determine the best-fit line.

**d) Drug – excipient interaction by visual observation:**

Several important factors that should be considered while doing visual observations to identify drug-excipient and excipient-excipient interactions include whether there are any physical changes, such as colour changes, phase separation, precipitation, or crystallisation. Next, texture and consistency should be noted, including any changes in the mixture's consistency and whether it becomes sticky, hard, or brittle. There are factors related to physical states, such as efflorescence, deliquescence, and hygroscopicity. There should not be the creation of clumps or aggregates. Odour changes or the creation of new smells may be signs of chemical breakdown or reactions. There should not be any signs of sedimentation or phase separation. Potential interactions that could impact the final pharmaceutical product's stability, efficacy, and safety can be found by keeping account of these factors.

**e) Melting point:**

The melting point of RES was determined using the capillary method. It was filled in a small quantity in a capillary which was inserted in melting point apparatus (MR-VIS, Labindia, Mumbai, India) and as the temperature raised the melting point of the drug was noted. The temperature at which the drug started melting was noted and a temperature at which the drug was completely melted was noted. The melting point was reported as a temperature range.

**f) Partition coefficient:**

To evaluate the drug's hydrophilicity and lipophilicity, the partition coefficient must be determined. For this, the Shake Flask method was applied. A particular quantity of the medication that is RES was dissolved in a mixture of equal parts of octanol and distilled water in a flask. After agitating the flask to reach equilibration, phase separation was accomplished by allowing it to rest. UV spectrophotometry was used to determine the resveratrol amounts in both phases upon separation. The samples were scanned at 304 nm. With the obtained absorbance, the concentration was calculated. Using the following formula, the partition coefficient (K) was determined: (Cumming H and Rucker C, 2017)

$$K_{o/w} = C_o / C_w \qquad \text{(Eq 4.1)}$$

Where, K- partition coefficient

Co - concentration of resveratrol in organic solvent

Cw - concentration of resveratrol in distilled water.

**Preparation of liposomes:**

The lipid components, phoshatidylcholine and cholesterol, in various ratios, were dissolved in a minimal volume of a chloroform-methanol mixture (9:1 v/v) in a 50 mL round-bottom flask with gentle swirling. During preparation, resveratrol was incorporated into the lipid mixture. The flask was then connected to a rotary evaporator (Nutronics, India), and nitrogen gas was used to maintain an inert atmosphere.

A vacuum of approximately 700 mm Hg was applied to evaporate the organic solvent, leading to the formation of a thin lipid/cholesterol film on the flask walls. To dissolve this film, diethyl ether (3 mL per 66 µmol lipid) was added and vortexed. Subsequently, PBS (pH 6.4) was introduced as the aqueous phase, followed by vortexing and bath sonication (EIE Instruments Pvt. Ltd., India) at 4°C. Sonication was carried out for about 2–3 minutes until a stable water-in-oil (w/o) emulsion was formed.

The emulsion-containing flask was then reattached to the rotary evaporator while nitrogen gas was continuously purged, and the mixture was stirred. A low vacuum (~200 mm Hg) was gradually applied to evaporate the ether slowly. The process continued until a semisolid gel was formed. The flask was removed, and the contents were stirred to break the gel. The vacuum pressure was then increased to approximately 300–350 mm Hg and maintained for 15 minutes. As most of the ether evaporated, the gel transitioned into a smooth suspension.

The flask was removed again, and the contents were mixed thoroughly. To eliminate any remaining ether, the vacuum pressure was gradually increased to 700 mm Hg and maintained for 30 minutes. The liposomes were then extruded, and the unentrapped drug was separated. The liposomal suspension was filtered using a nylon membrane filter with a 5 mm pore size. To isolate the free drug from the encapsulated drug, the filtrate was centrifuged at 10,000 rpm at 4°C for 90 minutes using a refrigerated centrifuge. The supernatant was discarded, and the pellet was re-dispersed in PBS (pH 6.4) before being stored in airtight glass containers at 4°C.

**Table: Batches prepared using various concentrations of drug and lipid ratios**

| Formulations | Cholesterol: Phosphatidylcholine | Resveratrol (mg) |
|---|---|---|
| **B1** | 1:1 | 1 |
| **B2** | 1:2 | 1 |
| **B3** | 1:3 | 1 |
| **B4** | 1:4 | 2 |
| **B5** | 1:5 | 2 |

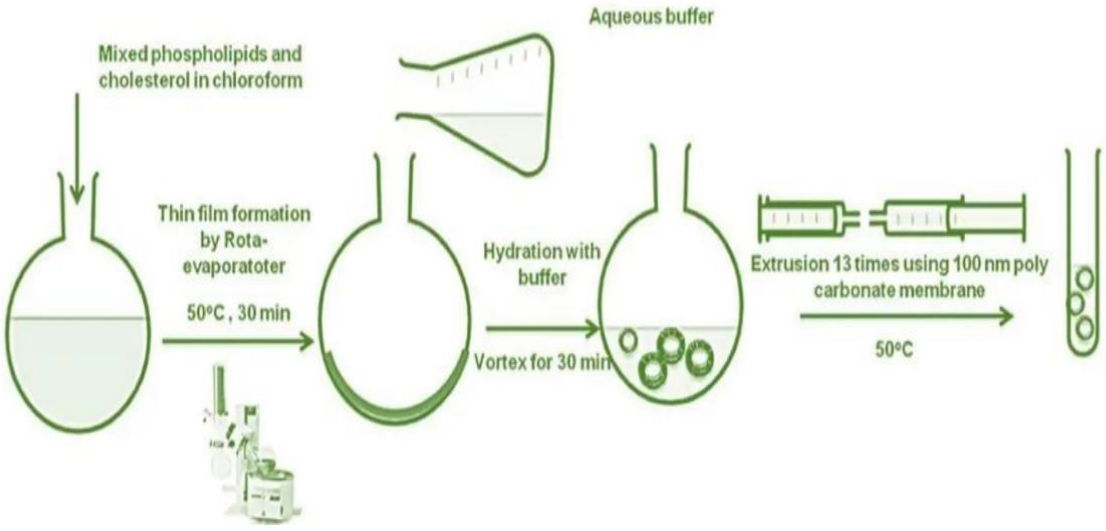


**Figure: Representation of the preparation of liposomes**

**Characterization of liposomes:**

**Determination of mean particle size, polydispersity index (PDI) and zeta potential:**

The mean particle size (z-average) of the liposomes and the polydispersity index (PDI), which indicates the width of the particle size distribution, were determined using photon correlation spectroscopy (PCS) with a Zetasizer (Nano ZS 90, Malvern Instruments, UK) at 25°C and a 90° scattering angle. To reduce opalescence before measurement, the liposomal formulation was diluted with double-distilled water.

The surface charge of the liposomes was evaluated by measuring the zeta potential, calculated using the Smoluchowski equation, with the same equipment at 25°C under an electric field strength of 23 V/cm. Each sample underwent three independent measurements, and all analyses were conducted 24 hours after preparation.

**Determination of entrapment efficiency:**

After centrifugation, the clear supernatant was carefully separated and analyzed for resveratrol content using a UV spectrophotometer at 304 nm after appropriate dilution with phosphate-buffered saline (PBS) at pH 6.4. This measurement determined the amount of unentrapped drug.

The liposomal pellet was then re-dispersed in PBS (pH 6.4), lysed with 2% Triton X-100, and sonicated for 10 minutes. The concentration of resveratrol was measured after appropriate dilution in phosphate buffer (pH 6.4) at 304 nm using a UV-visible spectrophotometer.
The drug entrapment efficiency (% EE) of resveratrol in each formulation was calculated using the following equation:

**%EE = [(Q- $Q_0$ / Q] × 100**
**Where:**

- **Q** is the amount of resveratrol measured in the liposomes.
- **$Q_0$** is the initial amount of resveratrol added to the liposomes.

**In-vitro drug release study**
The in vitro release of resveratrol from the optimized quercetin liposomes was evaluated using a diffusion cell apparatus (EMFD-08, Orchid Scientific & Innovative India Pvt. Ltd., Nasik, Maharashtra, India) with a dialysis membrane (molecular weight cutoff: 10,000 Da). Before use, the membrane was soaked in double-distilled water for 24 hours.
A 2 mL aqueous dispersion of resveratrol liposomes were placed in the donor compartment, while the receptor compartment was filled with a phosphate buffer (pH 7.4) as the dissolution medium. The system was maintained at 35 ± 0.5°C with continuous stirring at 100 rpm. Samples of 2 mL were withdrawn at specific time intervals (0, 1, 2, 3, 4, 5, 6, 12, 16, and 24 hours), filtered, and immediately replaced with an equal volume of fresh buffer. The collected samples were appropriately diluted, and analysed using UV-spectrometer at a wavelength of 304 nm.

**Stability of liposomes**
Information on the stability of drug substance is an integral part of the systematic approach to stability evaluation. Stability is defined as the extent to which a product remains within specified limits throughout its period of storage and use. A drug formulation said to be stable if it fulfils some requirements.

Procedure: From the five batches of liposomes prepared, the selected batch, was further tested for stability studies. The selected batch were divided into 3 sets and stored at:

- 4°C
- 30º C ± 2º C/60% RH ± 5% RH in humidity control oven (GINKYA IM 3500 series).
- 37°c 65% RH

The observations were made based on the basis of change in particle size, PDI, Zeta potential and change in the encapsulation efficiency.

## RESULTS AND DISCUSSION:

### *5.1 Preformulation studies*

**5.1.1 Organoleptic properties** The drug powder was physically examined and the following observations were recorded. The recorded observations of physical state, colour and powder odour of the drug were found to be similar to the reference reported in official literature.

**Table 5.1: Observed organoleptic properties of Resveratrol**

| **Properties** | Resveratrol |
|---|---|
| **Physical form** | Amorphous powder |
| **Colour** | Off - white |
| **Odor** | Odourless – slight earthy smell |

**5.1.2 Solubility studies**: In solvents: It was experimentally found that resveratrol had highly soluble in methanol and the resultant order of solubility is methanol>ethanol>DMSO. In excipients: Using UV/VIS spectroscopy, the solubility of resveratrol in a variety of excipients. Drug was found to be soluble in phosphatidylcholine, cholesterol and tween 80, hence these excipients are selected to be used in formulation development.

**Table 5.2: Experimentally obtained solubility values of resveratrol in different excipients**

| **Excipients** | **Concentration** |
|---|---|
| Methanol | 6.286 ± 0.16 mg/ml |
| Ethanol | 5.147 ± 0.15 mg/ml |
| DMSO | 3.289 ± 0.29 mg/ml |
| Phosphatidylcholine | 8.974 ± 0.51 mg/ml |
| Cholesterol | 9.487 ± 0.26 mg/ml |
| Tween 80 | 10.408 ± 0.83 mg/ml |

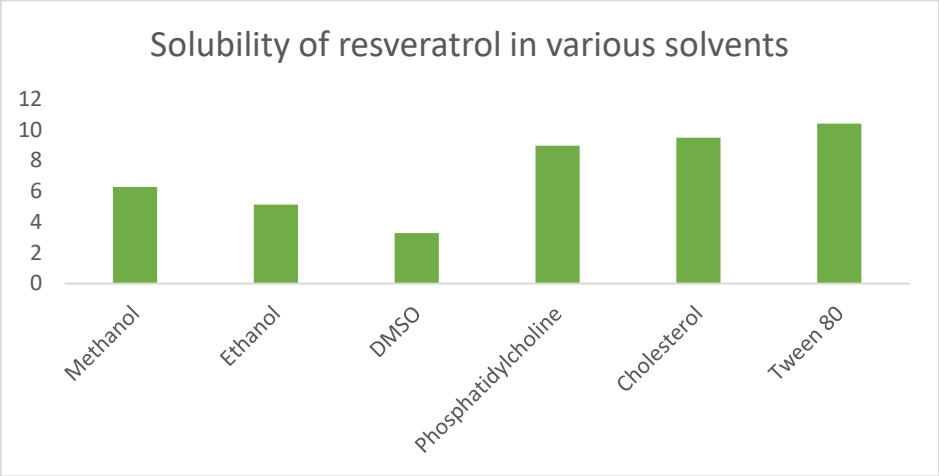


**Determination of Absorption maxima (λmax) and construction of Calibration curve of Resveratrol:**

**5.1.3.1.A Determination of Absorption maxima (λmax) of Resveratrol:**

Lambda max of resveratrol was identified using UV-Vis spectroscopy and was found to be 304 nm as depicted by the figure. The wavelength of 304 nm was chosen for the λmax because it is the point on a bell-shaped peak where the maximum absorption occurs. Selecting a peak with a bell shape is beneficial since the absorbance of a solution changes quickly with small wavelength differences on its steep sides. If there is even a slight variation in the wavelength setting of the instrument, this quick change can result in significant measurement inaccuracies. As a result, a bell-shaped peak reduces the possibility of appreciable errors in absorbance readings, guaranteeing more accurate and consistent observations.

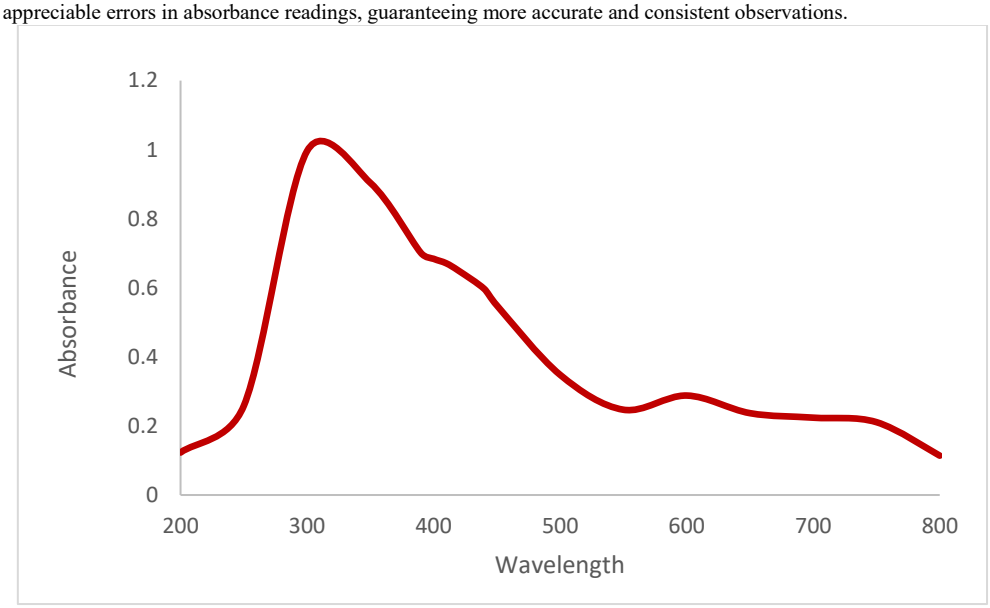


**Figure : Absorption maxima of resveratrol in Methanol Solvent Absorption maxima (λ max)**

**5.1.3.1.B Construction of calibration curve of Resveratrol:**

Using the different dilutions that were made, absorbance values of Resveratrol at different concentrations were determined and these values along with concentration values were plotted on a graph to get the calibration curve. The regression value was calculated and was found to be 0.986.

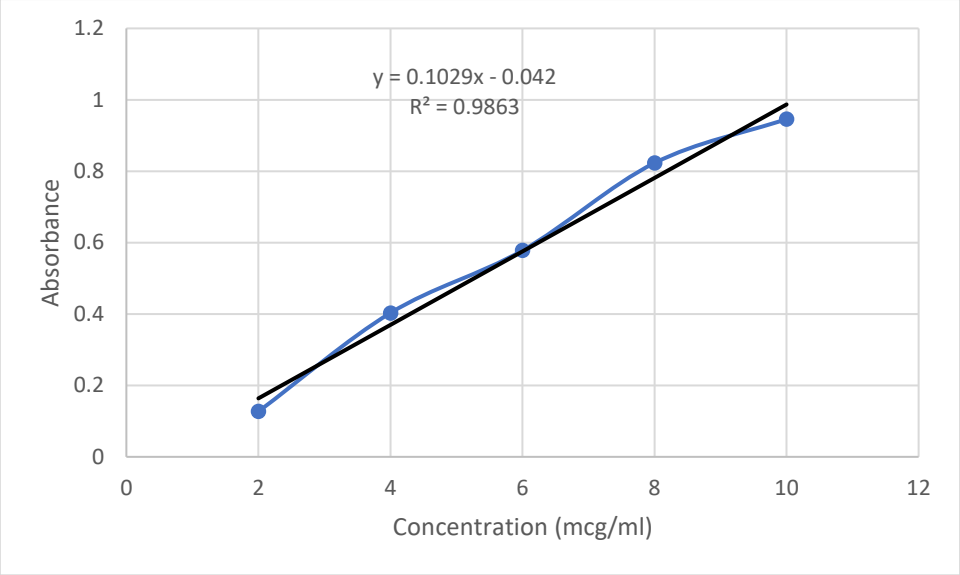


**Figure 5.3 depicts the generated calibration curve of Resveratrol in methanol.**

**5.1.3.1.C Construction of calibration curve of Resveratrol in PBS (pH 5.5):**

Using the different dilutions that were made in PBS of pH 5.5, absorbance values of Resveratrol at different concentrations were determined and these values along with concentration values were plotted on a graph to get the calibration curve. The regression value was calculated and was found to be 0.9837. Figure depicts the prepared calibration curve of Resveratrol in PBS (pH 5.5).

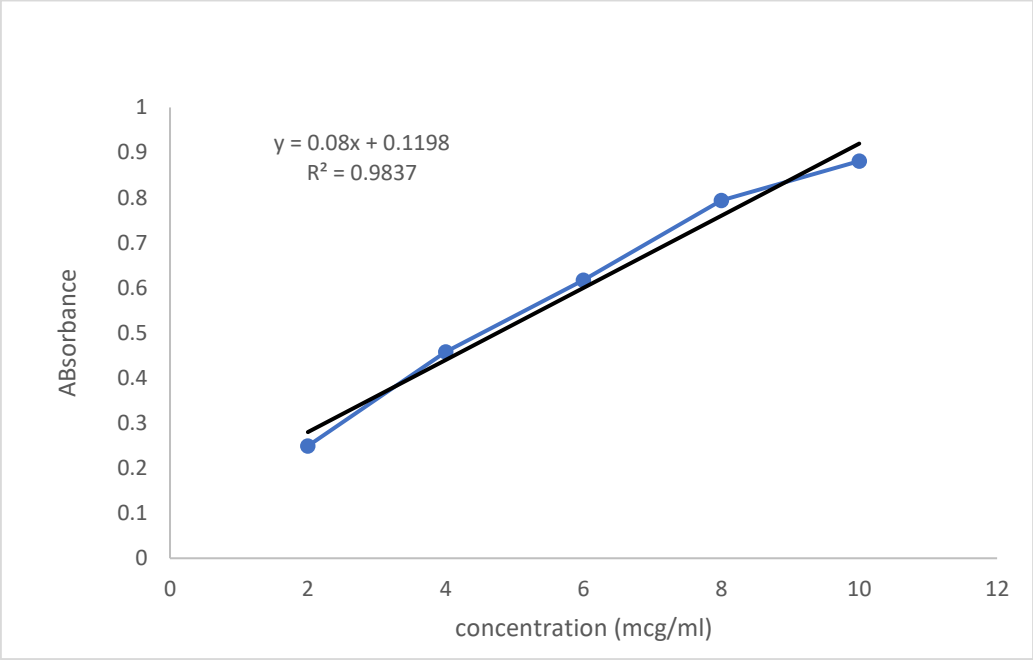


**Figure: Calibration curve of resveratrol in PBS**

**5.1.4 Drug – excipient interaction by visual observation:**

There were no physical changes, such as colour changes, phase separation, precipitation, or crystallisation. Texture and consistency were also same. No aggregates formation was there. Any new odour was not developed and there was no change in odour with absence of sedimentation or phase separation. These results suggested that the developed formulation is free of any kind of potential interactions and is stable and safe.

**5.1.5 Melting point:**

The melting point of pure Resveratrol was found to be 251 ± 2°C. Since the experimentally obtained melting point is found to be near the actual melting point of Resveratrol, it can be suggested that the compound is pure and this is also likely to be confirming the identity of the compound.

**5.1.6 Partition coefficient:**

To evaluate the drug's hydrophilicity and lipophilicity, the partition coefficient was determined because it is a fundamental parameter which can influence various parameters of formulation development like, solubility, permeability, stability, distribution and more. Absorbance values were determined using UV spectrophotometer of Resveratrol in octanol and Resveratrol in water, which was used to calculate concentration of Resveratrol in these solvents and the formula was used to determine partition coefficient, which was found to be 2.98 ± 0.08.

**Table 5.6: Mean absorbance with obtained concentration and calculated partition coefficient**

| Solvents | Mean absorbance ± SD(N=3) | Concentration ± SD(N=3) |
|---|---|---|
| Octanol | 0.189 ± 0.002 | 4.71 ± 0.13 |
| Water | 0.154 ± 0.004 | 1.58 ± 0.07 |
| Calculated partition coefficient (P) = 2.98 ± 0.08 | | |

**FTIR OF liposomes**

The spectra of liposomes align with the characteristics of intact liposomes, particularly in relation to the structure of phosphatidylcholine. The broad band centered at 3369 cm−1 corresponds to O–H stretching from water molecules associated with the liposome membranes through hydrogen bonding. Sharp bands observed between 3000-2800 cm−1 represent C–H stretching modes, with prominent peaks at 2925 cm−1 and 2854 cm−1 attributed to the symmetric and antisymmetric stretching vibrations of CH2 groups in alkyl chains, respectively. Additionally, the minor peak at 2959 cm−1 is linked to the antisymmetric stretch of terminal CH3 groups.

The shoulder-like band at 1729 cm−1 corresponds to the stretching vibration of ester C=O groups, characteristic of unsaturated diacyl lipids, as previously reported by Popova and Hincha (2016). The broader, stronger band at 1640 cm−1 is associated with the stretching vibration of C=C bonds in unsaturated aliphatic groups within fatty acid chains. At lower frequencies, the band at 1464 cm−1 corresponds to the scissoring bending vibrations of CH2 groups. Furthermore, characteristic vibrations of phosphate groups in the polar head are observed, including the PO2− antisymmetric stretch at 1219 cm−1 and the PO2− symmetric stretch at 1082 cm−1.

These major bands are consistent with those reported in the literature by Hasan et al. (2016) and Pawlikowska-Pawłęga et al. (2013). For a comprehensive summary, presents a schematic illustration of the key infrared bands identified in the FTIR analysis, corresponding to functional groups in the phosphatidylcholine structure**.**

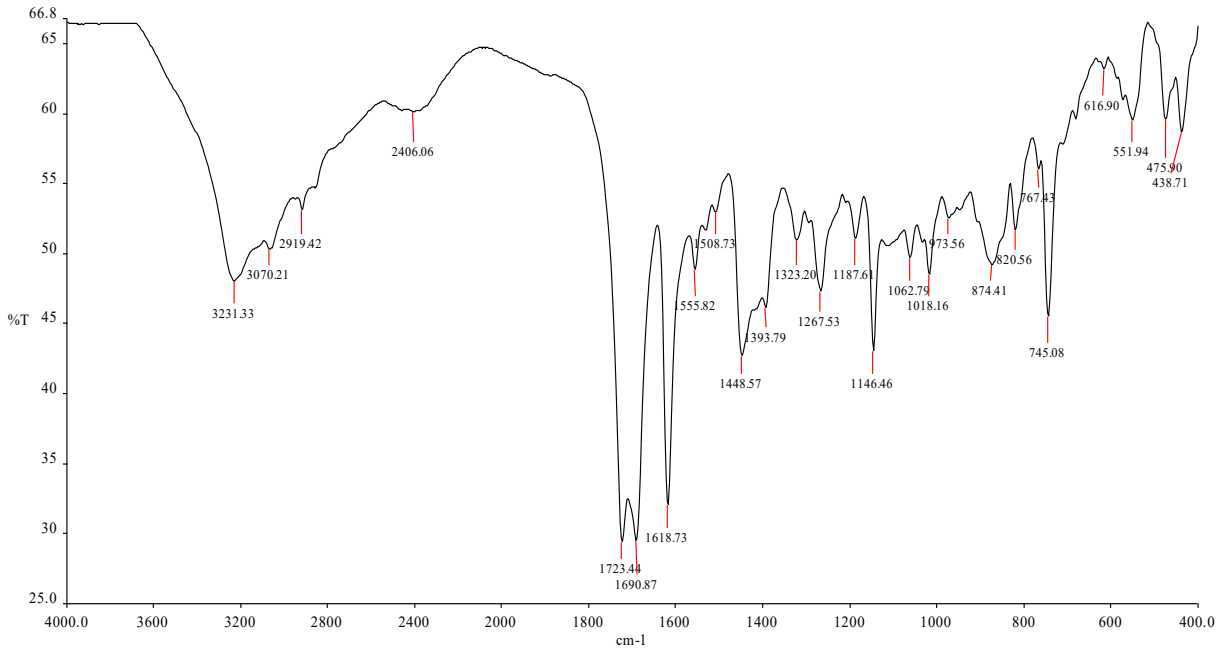


**Particle Size Distribution**

The average size and distribution of liposomes are crucial parameters, particularly when intended for therapeutic applications via inhalation or parenteral routes. Various techniques are available to assess submicrometer liposome size and distribution, including microscopy methods, size-exclusion chromatography (SEC), field-flow fractionation, and static or dynamic light scattering.

Several electron microscopy (EM) techniques, such as transmission EM with negative staining, freeze-fracture TEM, and cryo-EM, provide valuable insights into liposome morphology and allow visualization of particles of different sizes. However, these methods require the removal of liposomes from their native environment, making sample preparation complex. Additionally, they may introduce artifacts, cause shrinkage and shape distortion, and require significant time to obtain a representative size distribution. As a result, these techniques are not well-suited for routine measurements.

Dynamic Light Scattering (DLS), also known as Photon Correlation Spectroscopy, is commonly used to analyze liposome size distribution. This technique measures fluctuations in light scattering caused by particles undergoing Brownian motion. Through DLS, parameters such as particle size, polydispersity index (PDI), and zeta potential can be determined.

Particle size plays a critical role in the diffusion of particles through the stratum corneum. Studies have shown that smaller particles, around 50 nm, diffuse more effectively than larger particles, such as those measuring 200 nm. For instance, liposomes with a particle size of 120 nm demonstrated significantly higher accumulation of a loaded compound in the stratum corneum (72.88 ± 1.69%) and deeper layers of skin (0.76 ± 0.8%) compared to liposomes with sizes of 191 nm, 377 nm, and 810 nm. These larger particles showed 1.12-, 1.19-, and 1.83-fold lower concentrations in the stratum corneum and 4.68-, 7.29-, and 33.57-fold lower concentrations in deeper skin layers, respectively. While these findings highlight the influence of particle size, further research is needed to fully understand the relationship between particle size and skin permeability.

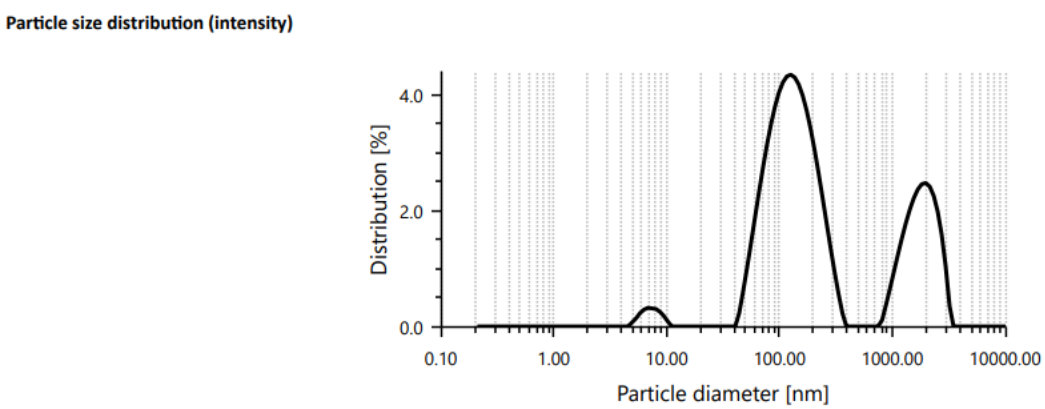


**Zeta potential**

The zeta potential of resveratrol-loaded liposomes was measured to evaluate the surface charge and colloidal stability of the formulation. The results indicated that the liposomes exhibited a negative zeta potential (-11.8 mV), which can be attributed to the presence of phospholipids and other anionic components in the lipid bilayer. This negative charge is essential for electrostatic repulsion between particles, preventing aggregation and ensuring the stability of the liposomal dispersion over time.

A zeta potential value greater than ±30 mV is generally considered indicative of a stable colloidal system due to sufficient repulsive forces preventing particle aggregation. The measured zeta potential of the resveratrol-loaded liposomes suggests that the formulation possesses adequate stability, reducing the likelihood of coalescence and sedimentation. Additionally, the surface charge influences interactions with biological membranes, potentially impacting cellular uptake and bioavailability.

The incorporation of resveratrol into liposomes may have slightly altered the zeta potential compared to blank liposomes due to interactions between the drug and lipid components. These interactions can affect the packing and orientation of lipid molecules, thereby modifying the surface charge. The Smoluchowski equation was used to calculate the zeta potential, ensuring accurate assessment under standardized conditions.

Overall, the observed zeta potential confirms the stability and suitability of the liposomal formulation for drug delivery applications. However, further studies on long-term stability and interactions with biological fluids are recommended to optimize the formulation for enhanced in vivo performance.

**Encapsulation efficiency**

**(**EE) refers to the proportion of core material successfully encapsulated within liposomess. Since liposomes can carry both hydrophobic and hydrophilic molecules, EE must be determined for all compounds encapsulated in the vesicles. EE is calculated as the difference between the total amount of the compound added for encapsulation and the amount of non-encapsulated compound, divided by the total compound added. This measure reflects the effectiveness of the encapsulation process and the quality of the liposomes.

Encapsulation efficiency can vary based on the physical state of the compound.

The experiment was performed and using the equation entrapment efficiency of the developed and finalized Resveratrol loaded liposomes was determined. The Entrapment Efficiency was found to be 68.72 ± 2.37%. This suggests that a good amount of drug was entrapped in the liposomal formulation.

**In-vitro drug release study:**

The in vitro drug release study of resveratrol-loaded liposomes was conducted to evaluate the release profile and sustained release potential of the formulation. The results demonstrated a biphasic release pattern, with an initial rapid release followed by a sustained release phase. The initial burst release can be attributed to the diffusion of resveratrol present on the surface or weakly associated with the liposomal bilayer. This phase is crucial for providing an immediate therapeutic effect.

Following the initial burst, a controlled and sustained release of resveratrol was observed over an extended period, indicating effective encapsulation within the liposomal bilayer. The slow-release phase can be attributed to the gradual diffusion of resveratrol from the lipid matrix and the structural

integrity of the liposomes, which act as a reservoir system. The sustained release is advantageous for enhancing the bioavailability and stability of resveratrol, which is otherwise susceptible to degradation under physiological conditions.

The dialysis membrane technique employed in this study ensured that the release kinetics were diffusion-controlled. The release profile was influenced by several factors, including lipid composition, particle size, and the nature of the dissolution medium. The use of phosphate buffer (pH 7.4) mimicked physiological conditions, allowing for a better understanding of the potential in vivo behavior of the liposomal formulation.

The prolonged release observed suggests that liposomal encapsulation can effectively modulate the release of resveratrol, reducing the frequency of administration and potentially enhancing therapeutic efficacy. Future studies should focus on correlating in vitro release data with in vivo pharmacokinetic studies to confirm the translational potential of the formulation.

The liposomes with Resveratrol was tested for release of drug and the medium used was PBS of pH 5.5. It was found after the experiment that the release of drug from the liposome is good and the drug is being released at a constant rate. The time of release was extended and about **86.49 ± 0.49%** of drug was calculated to be released in 10 hours. It was also noted that about 51.84 ± 0.14% of drug was released within 3-4 hours which was suggesting that a liposomal formulation can be considered to further sustain the release of drug from formulation.

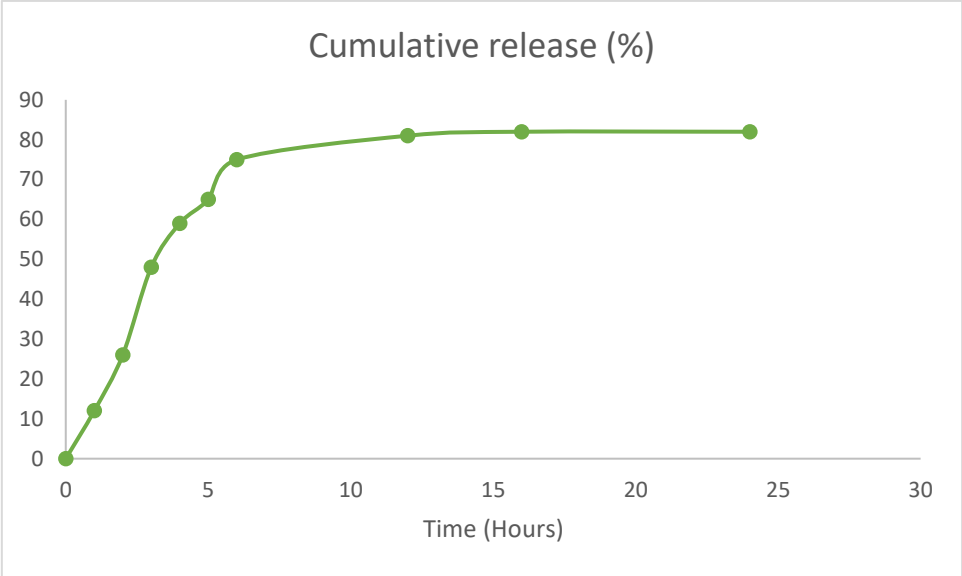


**Figure: percentage cumulative release of resveratrol from liposomes**

**Stability study**

Stability study of three samples of developed Resveratrol loaded organogel was done at a high temperature of 40°C and it was found that the pH of the formulation was consistent with negligible change, appearance does not changed in any manner to suggest any instability in the developed formulation as it was consistent throughout the test period and no change in colour, odour and consistency. Assay of drug was done and it was found that a very minor variation in the concentration of drug was there which did not suggest any degradation of the drug. The results suggests that all the samples of developed formulation did not show any major variations in pH, appearance and drug concentration which provides us evidence to report that the developed formulation is stable and it can be concluded that it is safe to use and its efficacy is also ascertained.

**Table: Results of stability studies**

| Parameter | Time point | Mean diameter | Zeta potential | %EE |
|---|---|---|---|---|
| **Set 1** (4°C) | **Week 0** | 258.47 | -11.56 | 69.54 |
| | **Week 2** | 266.38 | -14.57 | 64.75 |
| | **Week 4** | 389.95 | -18.59 | 64.32 |
| **Set 2** (30º C ± 2º C 60% RH ± 5% RH) | **Week 0** | 264.87 | -10.98 | 68.79 |
| | **Week 2** | 278.59 | -15.89 | 66.52 |
| | **Week 4** | 379.54 | -17.46 | 61.59 |
| **Set 3** (37° C ± 2º C 65% RH ± 5% RH) | **Week 0** | 251.49 | -11.28 | 68.97 |
| | **Week 2** | 273.54 | -13.68 | 63.51 |
| | **Week 4** | 305.87 | -17.54 | 60.35 |

**REFERENCES:**


1. Allen, T.M. · Cullis, P.R. Liposomal drug delivery systems: from concept to clinical applications *Adv. Drug Deliv. Rev.* 2013; 65:36-48
2. Alshaer, W. · Hillaireau, H. · Vergnaud, J. ... Functionalizing liposomes with anti-CD44 aptamer for selective targeting of cancer cells *Bioconjugate Chem.* 2015; 26:1307-1313
3. Amarandi, R.-M., A. Ibanescu, et al. (2022). "Liposomal-Based Formulations: A Path from Basic Research to Temozolomide Delivery Inside Glioblastoma Tissue." 14(2): 308.
4. Antoniou, A.I. · Giofrè, S. · Seneci, P. Stimulus-responsive liposomes for biomedical applications *Drug Discov. Today.* 2021; 26:1794-1824
5. Barenholz, Y., Doxil® the First FDA-Approved Nano-Drug: Lessons Learned, Journal of Controlled Release, Vol. 160, pp. 117-134, (2012)
6. Bigazzi, W. · Penoy, N. · Evrard, B.Supercritical fluid methods: an alternative to conventional methods to prepare liposomes *Chem. Eng. J.* 2019; 383:123106
7. Carugo, D. · Bottaro, E. · Owen, J. Liposome production by microfluidics: potential and limiting factors *Sci.Rep.* 2016; 6:25876
8. d'Avanzo, N. · Torrieri, G. · Figueiredo, P. LinTT1 peptide-functionalized liposomes for targeted breast cancer therapy *Int. J. Pharm.* 2021; 597:120346
9. Dikmetas, D. N., H. Yenipazar, et al. (2024). "Recent advances in encapsulation of resveratrol for enhanced delivery." 140475.
10. F. Lai, M. Schlich, C. Sinico, A.M. Fadda, Liposomes as Brain Targeted Delivery Systems, Nanomedicines for Brain Drug Delivery, Springer2021, pp. 29-59.
11. Federico, P., Vladimir, P.T., Recent Trends in Multifunctional Liposomal Nanocarriers for Enhanced Tumor Targeting. Journal of Drug Delivery, pp. 1-32, (2013).
12. Gkionis, L. · Aojula, H. · Harris, L.K. Microfluidic-assisted fabrication of phosphatidylcholine-based liposomes for controlled drug delivery of chemotherapeutics *Int. J. Pharm.* 2021; 604:120711
13. Has, C. · Sunthar, P. A comprehensive review on recent preparation techniques of liposomes *J. Liposome Res.* 2020; 30:336-365
14. He, K. · Tang, M.J.C.-b.i. Safety of novel liposomal drugs for cancer treatment *Adv. Prosp.* 2018; 295:13-19
15. Jaafar-Maalej, C. · Charcosset, C. · Fessi, H. A new method for liposome preparation using a membrane contactor *J. Liposome Res.* 2011; 21:213-220
16. Jiang, F. · Liu, B. · Lu, J. ...Progress and challenges in developing aptamer-functionalized targeted drug delivery systems*Int. J. Mol. Sci.* 2015; 16:23784-23822
17. Jin, E. · Zhang, B. · Sun, X. Acid-active cell-penetrating peptides for in vivo tumor-targeted drug delivery *J. Am. Chem. Soc.* 2013; 135:933-940
18. Li, M. · Zhao, G. · Su, W.-K. Enzyme-Responsive Nanoparticles for Anti-tumor Drug Delivery 2020
19. Lou, J. · Best, M.D. A general approach to enzyme-responsive liposomes *Chemistry.* 2020; 26:8597-8607
20. Sardana, K., A. Khurana, et al. (2021). "An exploratory pilot analysis of the optimal pellet number in 100 mg of itraconazole capsule to maximize the surface area to satisfy the Noyes–Whitney equation." 32(7): 788-794.
21. Sarris, A.H., Hagemeister, F., Romaguera, J., Rodriguez, M.A., McLaughlin, P., Tsimberidou, A.M., Medeiros, L.J., Samuels, B., Pate, O., Oholendt, M., Kantarjian, H., Burge, C., Cabanillas, F., Liposomal Vincristine in Relapsed Non-Hodgkin's Lymphomas: Early Results of an Ongoing Phase II Trial, Annals of Oncology, Vol. 11, No. 1, pp. 69-72, (2000).
22. Suk, J.S. · Xu, Q. · Kim, N. ... PEGylation as a strategy for improving nanoparticle-based drug and gene delivery *Adv. Drug Deliv. Rev.* 2016; 99:28-51
23. Torchilin, V.P. Recent advances with liposomes as pharmaceutical carriers, Nature reviews *Drug Discov.* 2005; 4:145-160
24. William, B. · Noémie, P. · Brigitte, E. Supercritical fluid methods: an alternative to conventional methods to prepare liposomes *Chem. Eng. J.* 2020; 383:123106
25. Wu, H. · Yu, M. · Miao, Y. Cholesterol-tuned liposomal membrane rigidity directs tumor penetration and anti-tumor effect *Acta Pharm. Sin. B.* 2019; 9:858-870